# Economic Resilience Under Disruption: A DIIM-Based Framework for Key Sector Identification in Singapore

**Yeoh Yu Yong**

**SCHOOL OF PHYSICAL AND MATHEMATICAL SCIENCES**

**A DISSERTATION SUBMITTED IN PARTIAL FULFILMENT OF THE REQUIREMENTS FOR THE DEGREE OF BACHELOR OF SCIENCE IN MATHEMATICAL SCIENCES**

**2026**

# Contents

# Abstract

This project develops a quantitative framework for assessing economic resilience under disruption using the Dynamic Inoperability Input-Output Model (DIIM) [1,2]. The DIIM captures how sectoral disruptions propagate through input-output linkages and how the economy recovers over time. Two disruption scenarios relevant to Singapore are studied: (1) the COVID-19 pandemic, using the 2019 input-output (IO) table aggregated to 15 sectors, and (2) a manpower disruption scenario motivated by potential grey zone conflicts that could trigger large-scale foreign worker departures, using the 2022 IO table with 107 sectors.

A central challenge in disruption management is identifying which sectors should receive priority intervention. The DIIM can identify these "key sectors" by simulating the full disruption and ranking sectors by economic loss, but this approach is computationally expensive and requires crisis-time data (initial inoperability $q_0$, demand perturbation $c^*$) that may not be available during the early stages of an event. This motivates the search for cheaper structural alternatives that use only the IO table.

This study evaluates five cheap methods—Principal Component Analysis (PCA) on the integrated IO matrix, backward linkage, forward linkage, output-weighted linkage, and network centrality—against the DIIM benchmark through Monte Carlo simulation (2 000 random $q_0$ vectors per scenario). Performance is measured by the ratio of economic loss reduction achieved by each cheap method relative to DIIM. For the 15-sector COVID scenario, output-weighted linkage matches DIIM in 89% of cases, and PCA matches in 86%. For the 107-sector manpower scenario, output-weighted linkage matches in 55% of cases, while PCA drops to only 5%. Logistic regression is used to derive decision rules that predict, from observable $q_0$ features, when each cheap method will perform adequately.

# Acknowledgement

I would like to express my sincere gratitude to my supervisor(s) for their guidance, encouragement, and constructive feedback throughout this project. Their expertise and patience were invaluable in shaping the direction of the work and in helping me develop my research and writing skills.

I am also grateful to the members of my committee and the faculty in the department for their insightful comments and support. I would like to acknowledge the technical and administrative staff whose assistance made it possible to carry out the practical aspects of this work.

I would like to thank my colleagues and friends for the discussions, collaboration, and encouragement that made the process both productive and enjoyable. Their willingness to share ideas and offer help at key moments is deeply appreciated.

Finally, I am profoundly thankful to my family for their unwavering support, understanding, and motivation. Their confidence in me has been a constant source of strength throughout my studies.

# Chapter 1

# Introduction

## 1.1 Background

Singapore is a small, open, city-state economy whose prosperity depends on deep integration with global supply chains and a large foreign workforce. Approximately one-third of Singapore's labour force consists of non-resident workers, spanning construction, manufacturing, marine shipyard, and services [3]. This dependence, while a source of economic dynamism, also constitutes a structural vulnerability: any event that rapidly reduces the available workforce—whether a pandemic, a geopolitical crisis, or a grey zone conflict—can propagate through interconnected sectors and inflict cascading economic losses far beyond the initially affected industries.

The COVID-19 pandemic demonstrated this vividly. When Singapore imposed the "circuit breaker" lockdown from 7 April to 1 June 2020 [4, 5], the disruption was not confined to directly affected sectors. Construction shutdowns deprived building-material manufacturers of demand, transport restrictions disrupted logistics, and hospitality closures cascaded into food supply chains. Understanding these cascading effects requires a framework that captures how sectors depend on each other and how disruptions propagate over time.

Beyond pandemics, Singapore faces national security scenarios that could produce similar or even more severe manpower disruptions. Grey zone conflicts—coercive actions below the threshold of conventional warfare, such as economic coercion, cyber attacks, or hybrid threats—could trigger rapid departures of foreign workers, disrupting sectors that rely heavily on non-resident labour [6]. Unlike COVID-19, where the external demand shock ($c^*$) was significant, a manpower disruption scenario is characterised by high initial inoperability ($q_0$) with $c^* = 0$, representing a purely structural disruption that propagates through the production network.

## 1.2 The Dynamic Inoperability Input-Output Model

The Inoperability Input-Output Model (IIM) and its dynamic extension (DIIM) provide a rigorous framework for modelling such disruptions [1]. Built on the Leontief input-output model, the DIIM measures "inoperability"—the normalised production loss of each sector on a scale from 0 (normal) to 1 (complete shutdown)—and simulates how initial shocks propagate through input-output linkages and how the economy recovers over time. The Shanghai COVID-19 study demonstrated the utility of this approach for quantifying sectoral vulnerability and evaluating risk management strategies [2].

## 1.3 The Key Sector Identification Problem

A critical application of the DIIM is identifying "key sectors"—those where targeted intervention (e.g., reducing inoperability by allocating recovery resources) yields the greatest reduction in total economic loss. The DIIM identifies these sectors by running the full dynamic simulation and ranking sectors by cumulative economic loss. However, this approach has two limitations:

1. **Computational cost**: The DIIM requires running the complete simulation for every candidate intervention strategy.
2. **Data requirements**: The DIIM needs crisis-time data—initial inoperability $q_0$ and the demand perturbation $c^*$—which may not be available in the early stages of a disruption or during pre-event planning.

This motivates the search for *cheap structural methods* that can identify key sectors using only the input-output table, which is available in peacetime. Principal Component Analysis (PCA) applied to the integrated IO matrix $H = A(I-A)^{-1}$ is one such method, previously shown to produce sector rankings comparable to DIIM for specific scenarios. However, whether PCA's performance generalises across different disruption profiles (i.e., different $q_0$ vectors) is an open question.

## 1.4 Objectives

This study addresses the following objectives:

1. Apply the DIIM framework to two disruption scenarios relevant to Singapore: the COVID-19 pandemic (15 sectors, 2019 IO table) and a manpower disruption (107 sectors, 2022 IO table).
2. Evaluate five cheap structural methods for key sector identification—PCA, backward linkage, forward linkage, output-weighted linkage, and network centrality—against the DIIM benchmark.
3. Determine the boundary conditions (in terms of the initial inoperability vector $q_0$) under which each cheap method can reliably substitute for the full DIIM simulation.
4. Derive practical decision rules that a policymaker can use to decide, given observable features of $q_0$, whether to use a cheap method or invest in running the full DIIM.

## 1.5 Report Organisation

Chapter 2 presents the methodology, including the derivation of the DIIM and the formulation of the cheap structural methods. Chapter 3 applies the DIIM to the COVID-19 scenario, presenting results and risk management analysis. Chapter 4 extends the analysis to the manpower disruption scenario. Chapter 5 compares the key sector identification methods across both scenarios. Chapter 6 develops the decision rules framework through Monte Carlo simulation and logistic regression. Chapter 7 discusses the implications, and Chapter 8 concludes.

# Chapter 2

# Methodology

This chapter presents the analytical framework. Section 2.1 derives the DIIM from the Leontief input-output model. Section 2.2 introduces the cheap structural methods for key sector identification. Section 2.3 defines the performance metric used to compare methods.

## 2.1 The Dynamic Inoperability Input-Output Model

### 2.1.1 Inoperability

This paper uses the DIIM model to assess the impacts of economic disruptions on the inoperability and economic losses of Singapore's sectors. The DIIM model is derived from the Leontief input-output model and is used to investigate the higher-order transmission effect of input-output linkages between sectors on inoperability. Using the DIIM model requires first introducing the concept of "inoperability", which is defined as follows:

$$\text{Inoperability} = \frac{\text{As Planned Production} - \text{Degraded Production}}{\text{As Planned Production}} \tag{2.1}$$

Where "As Planned Production" represents the output level of a sector under normal production, and "Degraded Production" represents the output level of a sector after being shocked in its production process. "Inoperability" takes values between 0 and 1, with higher values indicating greater damage to production caused by the shock. A value of 1 means the shocked sector has completely lost its production capacity, while a value of 0 means the sector is producing at a normal level.

### 2.1.2 From Leontief to IIM

Using the concept of inoperability defined above, the IIM model can be derived from the Leontief input-output model, as shown in Equation (2.2).

$$x = Ax + c \tag{2.2}$$

Where $x$ is the total output vector; $A$ is the technical coefficient matrix; $c$ is the final demand vector. If we define the output levels and the final demand vector of some shocked sectors as $\tilde{x}$ and $\tilde{c}$ respectively, then we can construct the input-output relationship between sectors after the shock.

Subtracting Equation (2.2) from the shocked-economy formulation:

$$x - \tilde{x} = A(x - \tilde{x}) + (c - \tilde{c}) \tag{2.3}$$

Defining $\hat{x}$ as a diagonalized matrix of the output vector and left multiplying $\hat{x}^{-1}$ on both sides of Equation (2.3):

$$\hat{x}^{-1}(x - \tilde{x}) = \hat{x}^{-1}A(x - \tilde{x}) + \hat{x}^{-1}(c - \tilde{c}) \tag{2.4}$$

Let $q = \hat{x}^{-1}(x - \tilde{x})$, $\quad A^* = \hat{x}^{-1}A\hat{x}$, $\quad c^* = \hat{x}^{-1}(c - \tilde{c})$; then Equation (2.5) can be derived, which is the IIM model.

$$q = A^* q + c^* \tag{2.5}$$

The details of each matrix in the IIM model are shown in Equations (2.6), (2.7), and (2.8):

$$q = \hat{x}^{-1}(x - \tilde{x}) = \begin{bmatrix} \frac{1}{x_1} & 0 & \cdots & \cdots & 0 \\ 0 & \ddots & & & \vdots \\ \vdots & & \frac{1}{x_i} & & \vdots \\ \vdots & & & \ddots & 0 \\ 0 & \cdots & \cdots & 0 & \frac{1}{x_n} \end{bmatrix} \begin{bmatrix} x_1 - \tilde{x}_1 \\ \vdots \\ x_i - \tilde{x}_i \\ \vdots \\ x_n - \tilde{x}_n \end{bmatrix} \tag{2.6}$$

$$A^* = \hat{x}^{-1}A\hat{x} = \begin{bmatrix} a_{11}\frac{x_1}{x_1} & \cdots & a_{1j}\frac{x_j}{x_1} & \cdots & a_{1n}\frac{x_n}{x_1} \\ \vdots & \ddots & \vdots & \ddots & \vdots \\ a_{i1}\frac{x_1}{x_i} & \cdots & a_{ij}\frac{x_j}{x_i} & \cdots & a_{in}\frac{x_n}{x_i} \\ \vdots & \ddots & \vdots & \ddots & \vdots \\ a_{n1}\frac{x_1}{x_n} & \cdots & a_{nj}\frac{x_j}{x_n} & \cdots & a_{nn}\frac{x_n}{x_n} \end{bmatrix} \tag{2.7}$$

$$\mathbf{c}^* = \hat{\mathbf{x}}^{-1}(\mathbf{c} - \tilde{\mathbf{c}}) = \begin{bmatrix} \frac{1}{x_1} & 0 & \cdots & 0 \\ 0 & \ddots & \ddots & \vdots \\ \vdots & \ddots & \frac{1}{x_i} & 0 \\ \vdots & & \ddots & \vdots \\ 0 & \cdots & \cdots & \frac{1}{x_n} \end{bmatrix} \begin{bmatrix} c_1 - \tilde{c}_1 \\ \vdots \\ c_i - \tilde{c}_i \\ \vdots \\ c_n - \tilde{c}_n \end{bmatrix} \tag{2.8}$$

### 2.1.3 The DIIM

The IIM model can be extended to the DIIM model by introducing a time variable and an elasticity coefficient matrix describing the recovery capacity of sectors. The discrete form of the DIIM model is:

$$q(t+1) = q(t) + K\left[A^* q(t) + c^*(t) - q(t)\right] \tag{2.9}$$

Where $K$ is the elasticity coefficient matrix describing the recovery capacity of sectors after being shocked in production. Assuming that the recovery capacity of a sector depends only on its own production, and is unrelated to the production linkages with other sectors, thus $K$ is a diagonal matrix with diagonal elements greater than 0. The larger the diagonal elements, the stronger the recovery capacity of the corresponding sector in response to shocks. $t$ is the discrete time variable, and $q(t)$ represents the sectoral inoperability vector at time $t$. Approximating Equation (2.9) to differential form:

$$\dot{q}(t) = K\left[A^* q(t) + c^*(t) - q(t)\right] \tag{2.10}$$

Solving Equation (2.10) we can get the equation describing the evolution of sectoral inoperability over time:

$$q(t) = e^{-K(I-A^*)t} q(0) + \int_0^t K e^{-K(I-A^*)(t-z)} c^*(z)\, dz \tag{2.11}$$

Assuming that the demand shock $c^*$ remains unchanged, and $c^* = 0$, then Equation (2.11) can be simplified to:

$$q(t) = e^{-K(I-A^*)t} q(0) \tag{2.12}$$

Where $q(0)$ represents the initial inoperability vector of sectors after being shocked. As time goes by, the inoperability changes at a rate of $e^{-K(I-A^*)t}$.

### 2.1.4 Initial Inoperability

The initial inoperability $q(0)$ is calculated as:

$$\text{Sector Initial Inoperability} = \frac{\text{Unavailable Workforce}}{\text{Size of Workforce}} \times \frac{\text{LAPI}}{\text{Sector Output}} \tag{2.13}$$

where the left factor is the proportion of unavailable workers in each sector and the right factor captures how dependent each sector is on labour as an input (Labour as a Proportion of Input, or LAPI).

### 2.1.5 Elasticity Coefficient

According to Equation (2.12), the inoperability of sector $i$ at time $t$ is:

$$q_i(t) = q_i(0) e^{-k_i(1-a^*_{ii})t} \tag{2.14}$$

From Equation (2.14), we can derive the calculation formula for $k_i$:

$$k_i = \frac{\ln[q_i(0)/q_i(T)]}{T_i(1-a^*_{ii})} \tag{2.15}$$

Where $q_i(0)$ is the initial inoperability of sector $i$; $q_i(T)$ is the inoperability of sector $i$ at time $T$; $a^*_{ii}$ is the element on the diagonal of matrix $A^*$, representing the self-dependence of sector $i$.

### 2.1.6 Economic Loss

Under the analytical framework of the DIIM model, the cumulative economic loss for sector $i$ is:

$$EL_i = x_i \int_{t=0}^{t=T} q_i(t)\, dt \tag{2.16}$$

Where $x_i$ is the planned output of sector $i$ under normal production.

## 2.2 Key Sector Identification Methods

A key sector is defined as one where targeted intervention—modelled as a 10% reduction in initial inoperability $q_0$—produces the largest reduction in total economic loss. Below we describe the expensive benchmark and five cheap structural alternatives.

### 2.2.1 DIIM-Based Identification (Benchmark)

The DIIM identifies key sectors by running the full simulation without intervention, then ranking sectors by their cumulative economic loss $EL_i$ from Equation (2.16). The top-$k$ sectors are selected for intervention. This is the "gold standard" but requires knowledge of $q_0$ and $c^*$.

### 2.2.2 PCA on the Integrated IO Matrix

Instead of using $A$ directly, this approach constructs the integrated input-output coefficient matrix:

$$H = A(I-A)^{-1} = A \cdot L \tag{2.17}$$

where $L = (I-A)^{-1}$ is the Leontief inverse. The matrix $H$ captures both direct and indirect effects through the production network. PCA is applied to $H$, and sectors are ranked by their Euclidean distance from the origin in the space of the first two principal components:

$$d_i^{\text{PCA}} = \sqrt{v_{i1}^2 + v_{i2}^2} \tag{2.18}$$

where $v_{i1}$ and $v_{i2}$ are the loadings of sector $i$ on PC1 and PC2 respectively. Sectors with larger $d_i^{\text{PCA}}$ are ranked higher.

### 2.2.3 Backward Linkage

Backward linkages measure the extent to which a sector draws on other sectors' outputs as inputs. They are calculated as the column sums of the Leontief inverse:

$$BL_j = \sum_{i=1}^{n} l_{ij} \tag{2.19}$$

where $l_{ij}$ are elements of $L$. A high $BL_j$ indicates that sector $j$ generates large demand for inputs from other sectors.

### 2.2.4 Forward Linkage

Forward linkages measure how much a sector's output is used as inputs by other sectors. They are calculated as the row sums of the Leontief inverse:

$$FL_i = \sum_{j=1}^{n} l_{ij} \tag{2.20}$$

A high $FL_i$ indicates that sector $i$ is an important supplier to the rest of the economy.

### 2.2.5 Output-Weighted Linkage

This method combines structural importance with economic size. The total normalised linkage for sector $i$ is:

$$TL_i = \frac{1}{2}\left(\frac{BL_i}{\overline{BL}} + \frac{FL_i}{\overline{FL}}\right) \tag{2.21}$$

where $\overline{BL}$ and $\overline{FL}$ are the mean backward and forward linkages. The output-weighted score is:

$$OWL_i = TL_i \times x_i \tag{2.22}$$

Sectors with high $OWL_i$ are both structurally important and economically large.

### 2.2.6 Network Centrality

The interdependency matrix $A^*$ is treated as the weighted adjacency matrix of a directed graph. Three centrality measures are computed and combined:

1. **Eigenvector centrality**: measures influence by accounting for the centrality of a sector's neighbours.
2. **PageRank**: measures importance based on the structure of incoming links, with a damping factor.
3. **Betweenness centrality**: measures how often a sector lies on the shortest path between other pairs of sectors.

Each measure is min-max normalised to $[0,1]$, and the composite score is:

$$NC_i = \widehat{EC}_i + \widehat{PR}_i + \widehat{BC}_i \tag{2.23}$$

where $\widehat{\cdot}$ denotes normalisation. Sectors with higher $NC_i$ are ranked higher.

## 2.3 Performance Metric

To compare a cheap method against DIIM, we define the *performance ratio*:

$$R_m = \frac{\Delta EL_m}{\Delta EL_{\text{DIIM}}} \tag{2.24}$$

where $\Delta EL_m$ is the total economic loss reduction achieved by intervening in the top-$k$ sectors identified by cheap method $m$, and $\Delta EL_{\text{DIIM}}$ is the reduction achieved by the DIIM's top-$k$ sectors. If $R_m \geq 0.95$, the cheap method is considered "close enough" to substitute for DIIM.

# Chapter 3

# Case Study 1: COVID-19 Pandemic

This chapter applies the DIIM framework to Singapore's COVID-19 pandemic, presenting the data, simulation results, and risk management analysis.

## 3.1 Data and Model Parameters

### 3.1.1 Input-Output Table

The IO transaction data for Singapore is obtained from the Department of Statistics, Singapore [7]. This study uses the 2019 IO table because it is the closest year before COVID-19 and represents the pre-pandemic baseline. The available IO table is aggregated into 20 broad sectors, and this study further aggregates them into 15 sectors to match the Ministry of Manpower dataset used to compute initial inoperability. The mapping is provided in Appendix A (Table 8.1).

From the aggregated IO table, the technical coefficient matrix $A$ is computed. A cross-section of $A$ is provided in Appendix A (Table 8.2).

### 3.1.2 Initial Inoperability

Initial inoperability is calculated using Equation (2.13). The workforce unavailability component is obtained from Ministry of Manpower data, and the labour dependence component is derived from the IO table. The initial inoperability values for the 15 aggregated sectors are listed in Appendix A (Table 8.3).

### 3.1.3 Model Parameters

Singapore's lockdown measures ("circuit breaker") were implemented from 7 April to 1 June 2020, which is 55 days [4, 5]. This study sets the shock duration to 55 days.

In late April 2022 (751 days after the start of lockdown), Singapore's DORSCON level was lowered from Orange to Yellow, and employees were allowed to return to workplaces. This study assumes a final inoperability $q_i(T_i) = 1\%$, meaning economic activity returns to 99% of pre-lockdown levels after 751 days.

## 3.2 Results

### 3.2.1 Inoperability Evolution

Figure 3.1 shows the simulated inoperability trajectories for the 15 aggregated sectors over the shock-and-recovery horizon. Inoperability rises during the shock window as disruptions propagate through input-output linkages, and it declines during recovery as sectors gradually restore production. Because sectors are interconnected, each sector experiences both direct effects from its own disruption and indirect effects transmitted from other sectors.

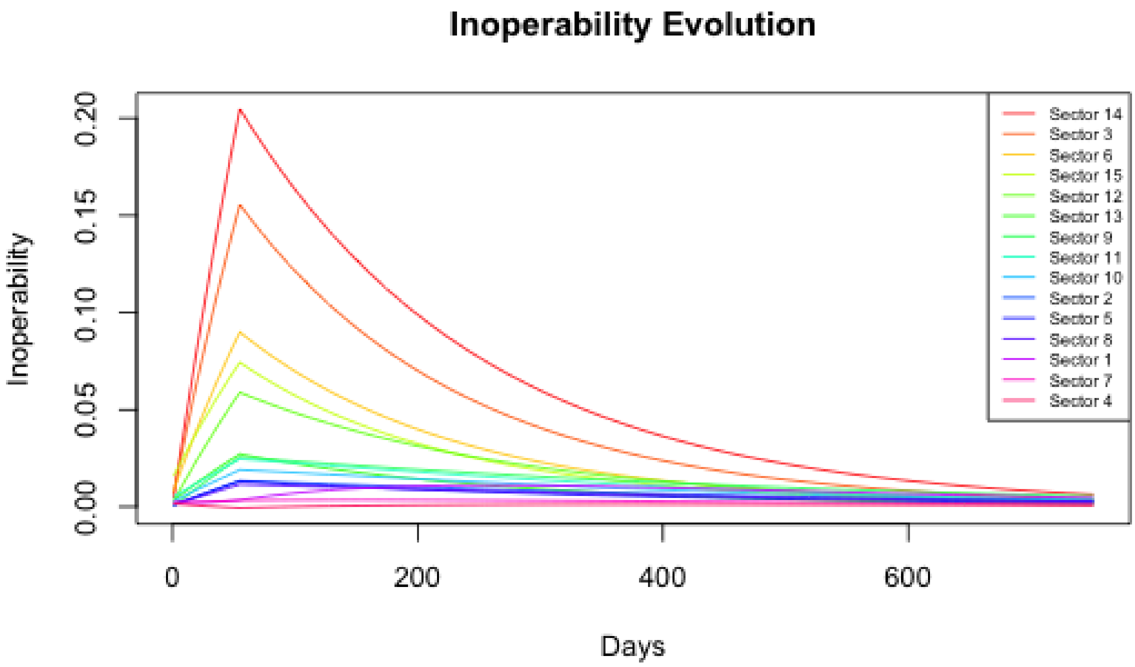


Figure 3.1: Inoperability evolution over the shock-and-recovery horizon (COVID-19, 15 sectors).

### 3.2.2 Economic Loss Evolution

Figure 3.2 presents the corresponding economic-loss evolution. Sectors with larger baseline outputs can accumulate large absolute losses even if their relative inoperability is not the highest, while smaller sectors may show high inoperability but smaller absolute losses.

### 3.2.3 Identifying Vulnerable Sectors

This section identifies vulnerable sectors using two measures: inoperability (relative production loss) and cumulative economic loss (absolute output loss). Figure 3.3 plots each sector using its rank in inoperability (y-axis) and its rank in economic loss (x-axis), so sectors that rank high in both measures are easy to identify.

To support prioritisation, we define ordinal "zones" (Top 5, Top 7, Top 10) as the intersection of sectors that appear in the top-*k* rankings of both measures. For example, the Top 5 zone contains sectors that are simultaneously ranked in the top five for both inoperability and economic loss, highlighting sectors that are both heavily disrupted and economically important.

Differences between the two rankings are expected. For example, a sector such as Arts, Entertainment & Recreation may rank high in inoperability but lower in economic loss if its baseline output is smaller than that of other sectors. Overall, Figure 3.3 provides a practical view for decision-making when policymakers want to balance restoring functionality (low inoperability) and reducing macroeconomic damage (low loss).

## 3.3 Sensitivity Analysis

To study the effect of lockdown duration, we simulate three lockdown lengths: 40, 55, and 70 days while keeping other parameters unchanged. Across sectors, longer lockdown durations lead to higher cumulative economic losses. The results also suggest the sector rankings of economic loss remain broadly

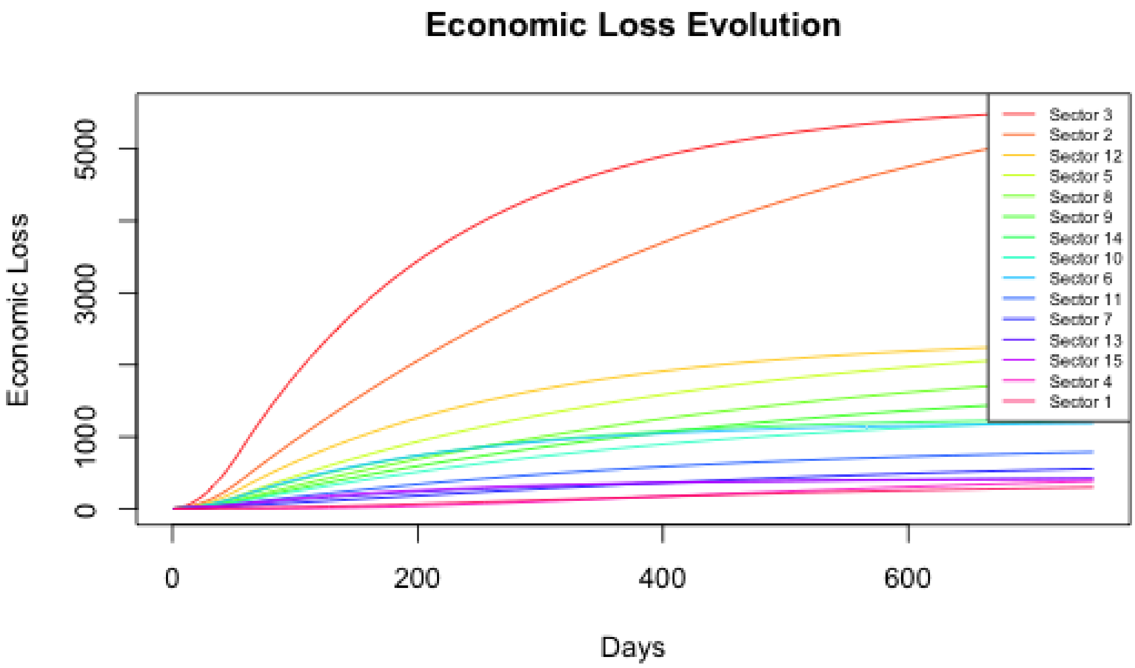


Figure 3.2: Economic loss evolution over the shock-and-recovery horizon (COVID-19, 15 sectors).

| | 2 | 3 | 5 | 12 | 8 | 9 | 10 | 14 | 6 | 11 | 7 | 13 | 15 | 4 | 1 |
|---|---|---|---|---|---|---|---|---|---|---|---|---|---|---|---|
| 14 | | | | | | | | X | | | | | | | |
| 3 | | X | | | | | | | | | | | | | |
| 6 | | | | | | | | | X | | | | | | |
| 12 | | | | X | | | | | | | | | | | |
| 15 | | | | | | | | | | | | | X | | |
| 9 | | | | | | X | | | | | | | | | |
| 13 | | | | | | | | | | | | X | | | |
| 11 | | | | | | | | | | X | | | | | |
| 2 | X | | | | | | | | | | | | | | |
| 10 | | | | | | | X | | | | | | | | |
| 5 | | | X | | | | | | | | | | | | |
| 8 | | | | | X | | | | | | | | | | |
| 1 | | | | | | | | | | | | | | | X |
| 7 | | | | | | | | | | | X | | | | |
| 4 | | | | | | | | | | | | | | X | |

| **Top 5 Zone** | |
|---|---|
| 3 | Construction |
| 12 | Public Administration & Education |

| **Top 7 Zone** | |
|---|---|
| 9 | Real Estate Services |

| **Top 10 Zone** | |
|---|---|
| 14 | Arts, Entertainment & Recreation |
| 6 | Accommodation & Food Services |
| 11 | Administrative & Support Services |
| 2 | Manufacturing |
| 10 | Professional Services |

Figure 3.3: Joint impact matrix: inoperability rank vs. economic loss rank (COVID-19).

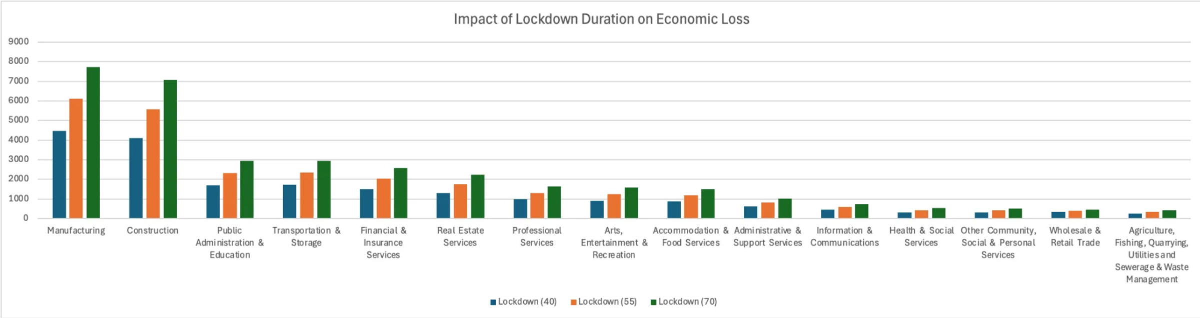


Figure 3.4: Total economic loss under different lockdown durations (COVID-19).

consistent under moderate changes in lockdown duration. Figure 3.4 shows the total economic loss for each sector under different lockdown durations.

## 3.4 Risk Management Analysis

This section evaluates risk management alternatives using the surrogate worth trade-off (SWT) method [8], focusing on the trade-off between investment costs and benefits measured as economic losses avoided.

### 3.4.1 Net Benefit

Net benefit for policy option $j$ is defined as:

$$\delta_j = \Gamma_{w[0]} - \Gamma_{w[j]} - \gamma_j \tag{3.1}$$

Here $\Gamma_{w[0]}$ is the baseline economic loss without policy, $\Gamma_{w[j]}$ is the economic loss under policy $j$, and $\gamma_j$ is the cost of implementing policy $j$.

### 3.4.2 Scenario 1 (Baseline): No Policy

In Scenario 1, no risk management measures are taken and the model results represent the baseline outcome. The execution cost is 0, and net benefit is set to 0 to serve as the comparison baseline.

$$\delta_0 = \Gamma_{w[0]} - \Gamma_{w[0]} - 0 = 0 \tag{3.2}$$

### 3.4.3 Scenario 2: Risk Control Investment

In this scenario, the government is assumed to spend 1 billion SGD in advance on risk control to reduce the pandemic impact. The policy is assumed to reduce the inoperability impact by 5% per day, meaning each day's inoperability is scaled to 95% of the original level before being used in the DIIM. Under this assumption:

$$\begin{aligned} \delta_1 &= \Gamma_{w[0]} - \Gamma_{w[1]} - \gamma_1 = 26\,967.3 - 2\,323.01 - 1\,000 = 23\,644.29 \text{ million SGD}, \\ \lambda_{12} &= \frac{\gamma_1}{\Gamma_{w[0]} - \Gamma_{w[1]}} = \frac{1\,000}{26\,967.3 - 2\,323.01} = 0.0406 \end{aligned} \tag{3.3}$$

### 3.4.4 Scenario 3: Lockdown Reduction

In this scenario, the government is assumed to spend 2 billion SGD in total. The additional spending is assumed to reduce the lockdown period from 55 days to 30 days:

$$
\begin{aligned}
\delta_2 &= \Gamma_{w[0]} - \Gamma_{w[2]} - \gamma_2 = 26\,967.3 - 17\,564.99 - 2\,000 = 7\,402.31 \text{ million SGD}, \\
\lambda_{12} &= \frac{\gamma_2}{\Gamma_{w[0]} - \Gamma_{w[2]}} = \frac{2\,000}{26\,967.3 - 17\,564.99} = 0.2127
\end{aligned}
\tag{3.4}
$$

### 3.4.5 Comparing Policies

Policy 1 obtains 1 SGD of benefit for each 0.041 SGD of investment cost, while Policy 2 obtains 1 SGD of benefit for each 0.21 SGD of investment cost. Under these assumptions, Policy 1 is preferred because it has a smaller cost per unit benefit. This demonstrates how the DIIM framework can support cost-benefit analysis of competing risk management strategies.

# Chapter 4

# Case Study 2: Manpower Disruption

This chapter extends the DIIM framework to a manpower disruption scenario motivated by Singapore's dependence on foreign labour and the potential for grey zone conflicts to trigger workforce departures.

## 4.1 Background: Singapore's Foreign Worker Dependence

Singapore's economy relies on approximately 1.4 million foreign workers, who constitute roughly one-third of the total labour force [3]. These workers are concentrated in sectors such as construction, manufacturing, marine shipyard, process industries, and domestic services. While this reliance on foreign labour has been a key enabler of economic growth, it creates a structural vulnerability to events that could trigger rapid workforce departures.

Grey zone conflicts—coercive actions that fall below the threshold of conventional warfare—represent a plausible threat scenario [6]. Such conflicts could include economic sanctions, cyber attacks on critical infrastructure, disinformation campaigns, or military posturing in the region. Any of these could erode confidence among foreign workers and their home governments, potentially triggering a significant and rapid outflow of non-resident workers.

Unlike the COVID-19 scenario, where disruption arose from both workforce unavailability ($q_0 > 0$) and reduced demand ($c^* > 0$), a manpower disruption is characterised by:

- **High initial inoperability** ($q_0 > 0$): Sectors lose productive capacity as workers depart.
- **No external demand shock** ($c^* = 0$): The disruption is purely structural. Demand may persist but cannot be met due to workforce shortages.

This distinction is important because the DIIM solution simplifies to $q(t) = e^{-K(I-A^*)t}q(0)$ when $c^* = 0$ (Equation (2.12)), meaning the disruption dynamics are governed entirely by the structure of the economy ($A^*$) and the initial shock ($q_0$).

## 4.2 Data and Model Parameters

### 4.2.1 Input-Output Table

This scenario uses the 2022 Singapore IO table, which provides a more granular sectoral breakdown of 107 sectors. The finer resolution is essential for capturing the heterogeneous distribution of foreign workers across sub-sectors.

### 4.2.2 Initial Inoperability

Initial inoperability is computed using the same method as Equation (2.13), with workforce unavailability data reflecting the proportion of foreign workers in each sector. Sectors with high foreign worker concentrations (e.g., construction, process industries) have correspondingly higher initial inoperability.

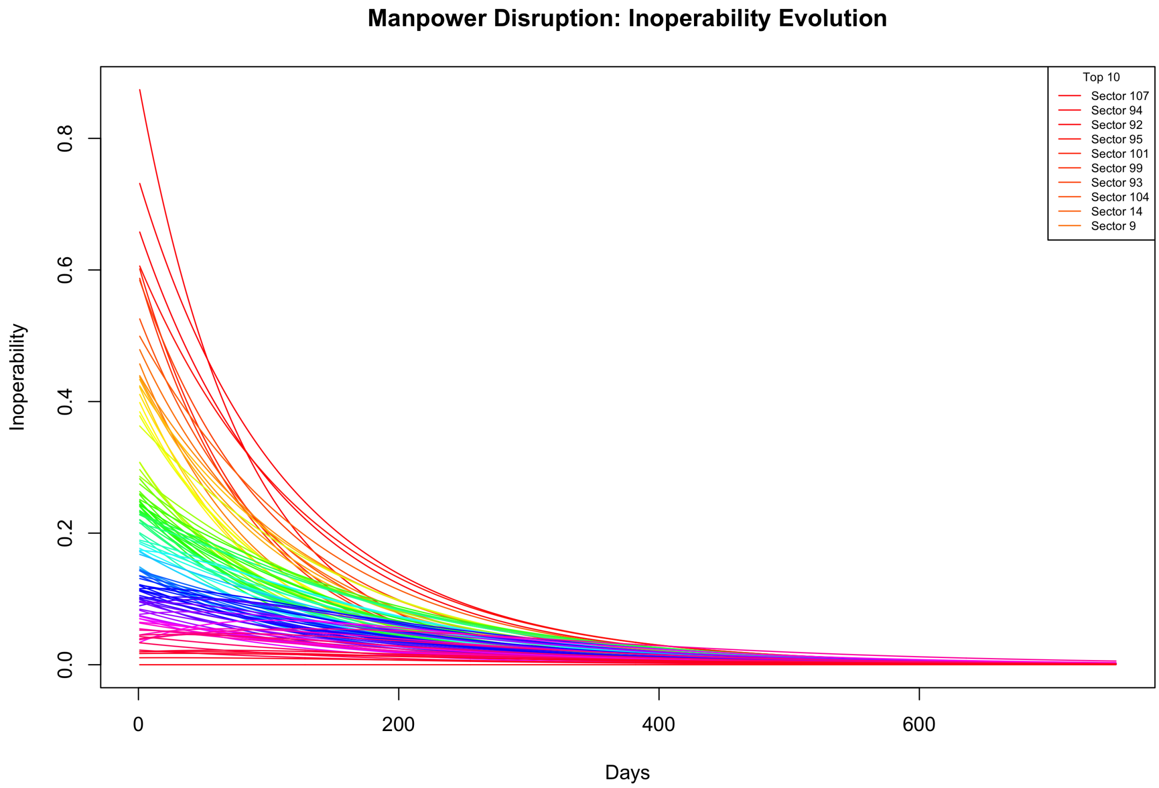


Figure 4.1: Inoperability evolution for the manpower disruption scenario (107 sectors).

### 4.2.3 Model Parameters

The shock duration is set to 55 days to enable comparison with the COVID-19 scenario, though a manpower disruption could have a different timeline. The total simulation horizon is 751 days with a final inoperability of 1%, representing near-full recovery through workforce replacement, retraining, or automation.

## 4.3 Results

### 4.3.1 Inoperability Evolution

Figure 4.1 shows the simulated inoperability trajectories for the 107 sectors. Compared to the COVID-19 scenario, the manpower disruption exhibits:

- Greater dispersion in initial inoperability across sectors, reflecting the uneven distribution of foreign workers.
- Stronger cascading effects through the 107-sector production network, as disruptions in labour-intensive sectors propagate to downstream industries.

### 4.3.2 Economic Loss Evolution

Figure 4.2 presents the cumulative economic loss evolution. The 107-sector resolution reveals that even sectors with moderate inoperability can accumulate substantial losses if their baseline output is large (e.g., manufacturing sub-sectors, financial services).

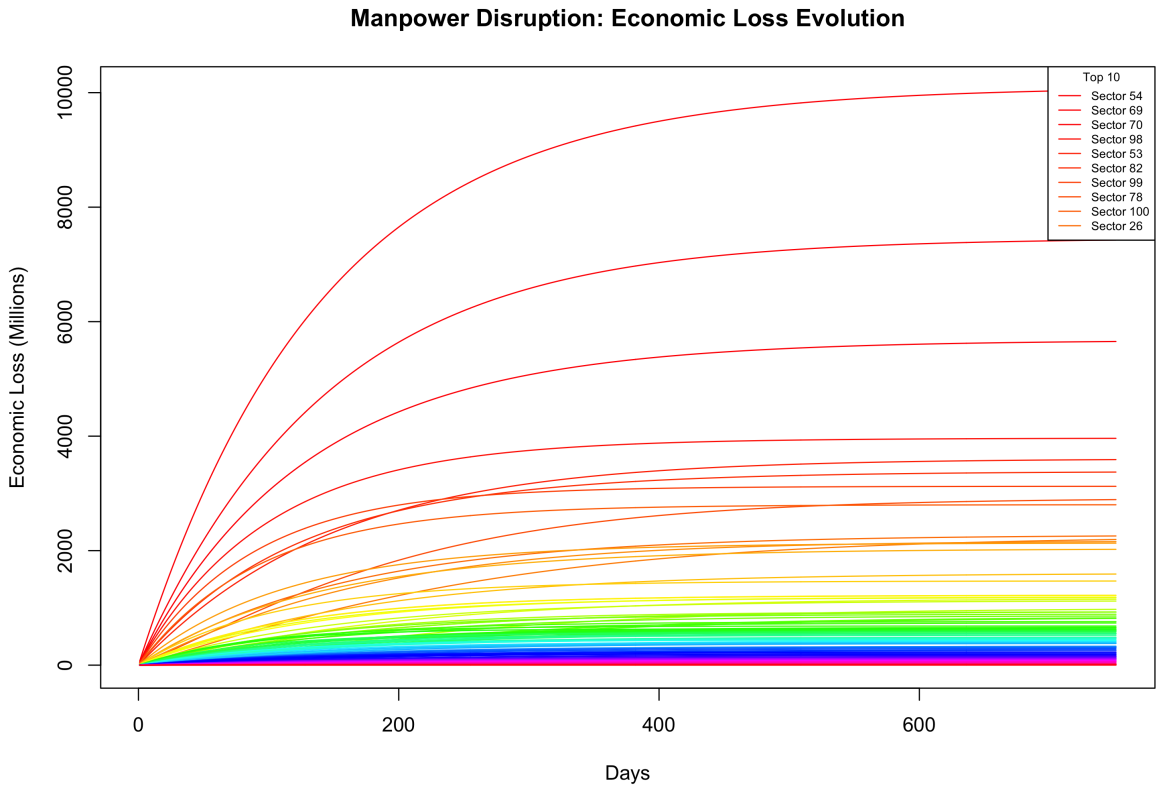


Figure 4.2: Economic loss evolution for the manpower disruption scenario (107 sectors).

## 4.4 Comparison with COVID-19

Table 4.1 summarises the key structural differences between the two scenarios.

The manpower scenario is structurally more complex because (1) the 107-sector economy has a denser and more heterogeneous interdependency matrix $A^*$, and (2) the absence of a demand shock means the entire disruption propagation is driven by the production network. These structural differences have important implications for the effectiveness of cheap key sector identification methods, as explored in the following chapters.

| **Parameter** | **COVID-19** | **Manpower** |
|---|---|---|
| Number of sectors | 15 | 107 |
| IO table year | 2019 | 2022 |
| Demand shock $c^*$ | $> 0$ | $= 0$ |
| Shock type | Demand + supply | Pure supply |
| Lockdown duration | 55 days | 55 days |
| Total horizon | 751 days | 751 days |

Table 4.1: Comparison of COVID-19 and manpower disruption scenario parameters.

# Chapter 5

# Key Sector Identification Methods

This chapter compares the key sector identification methods described in Chapter 2 using the actual disruption data from both case studies. Recall that the DIIM identifies key sectors by running the full simulation and ranking by economic loss (expensive, requires $q_0$ and $c^*$), while the cheap methods use only the IO table structure.

## 5.1 PCA Applied to the IO Matrix

PCA is applied to the integrated IO matrix $H = A(I - A)^{-1}$. Table 5.1 lists the PCA loadings for the COVID-19 scenario (15 sectors), sorted by Euclidean distance in the PC1–PC2 space.

| Sector ID | PC1 | PC2 | $d_i^{\mathbf{PCA}}$ |
|---|---|---|---|
| 3 | 0.773 | −0.159 | 0.789 |
| 2 | 0.489 | 0.548 | 0.734 |
| 5 | 0.231 | 0.602 | 0.645 |
| 8 | 0.174 | 0.320 | 0.364 |
| 4 | 0.164 | 0.198 | 0.257 |
| 10 | 0.141 | 0.185 | 0.233 |
| 7 | 0.107 | 0.232 | 0.256 |
| 11 | 0.100 | 0.154 | 0.184 |
| 1 | 0.082 | 0.203 | 0.219 |
| 9 | 0.066 | 0.120 | 0.137 |
| 12 | 0.021 | 0.034 | 0.040 |
| 6 | 0.019 | 0.040 | 0.044 |
| 15 | 0.010 | 0.016 | 0.019 |
| 14 | 0.004 | 0.006 | 0.008 |
| 13 | 0.002 | 0.004 | 0.005 |

Table 5.1: PCA loadings and Euclidean distance for COVID-19 sectors (15 sectors).

The top-5 PCA sectors for COVID-19 are sectors 3 (Construction), 2 (Manufacturing), 5 (Transportation & Storage), 8 (Financial & Insurance Services), and 4 (Wholesale & Retail Trade). These sectors have the largest loadings on the principal components that capture the dominant patterns of sectoral interdependence in the IO table.

For the manpower scenario (107 sectors), PCA is computed on the corresponding $H$ matrix. The top-5 PCA sectors are sectors 17, 57, 69, 54, and 62. These differ substantially from the COVID-19 PCA sectors because the 107-sector IO table has a different structure and more granular interdependencies.

## 5.2 Cheap Method Rankings

Table 5.2 and Table 5.3 show the top-5 sectors identified by each method for the two scenarios.

| Method | Top-5 Sectors (COVID-19) |
|---|---|
| PCA | 3, 2, 5, 8, 4 |
| Network Centrality | 4, 9, 8, 2, 10 |
| Backward Linkage | 3, 5, 1, 7, 6 |
| Forward Linkage | 2, 8, 3, 5, 7 |
| Output-Weighted Linkage | 2, 4, 5, 8, 7 |

Table 5.2: Top-5 sectors by each cheap method (COVID-19, 15 sectors).

| Method | Top-5 Sectors (Manpower) |
|---|---|
| PCA | 17, 57, 69, 54, 62 |
| Network Centrality | 54, 69, 78, 71, 70 |
| Backward Linkage | 51, 60, 17, 52, 62 |
| Forward Linkage | 54, 78, 69, 17, 57 |
| Output-Weighted Linkage | 54, 57, 69, 26, 70 |

Table 5.3: Top-5 sectors by each cheap method (Manpower, 107 sectors).

Several observations emerge:

1. **Method agreement varies**: For COVID-19, sectors 2 and 5 appear in most methods' top-5 lists, suggesting strong consensus on their structural importance. For manpower, sectors 54 and 69 are identified by multiple methods.
2. **PCA and forward linkage have the most overlap**: Both capture supply-side importance through eigenvector-based and row-sum-based measures respectively.
3. **Backward linkage is the most different**: It emphasises demand-pull importance (column sums), which captures a different dimension of sectoral influence.

## 5.3 Comparison at Original Disruption Data

Using the actual $q_0$ data from each scenario, we compare each cheap method's economic loss reduction against the DIIM benchmark when intervening in the top-5 sectors.

For the COVID-19 scenario, PCA and output-weighted linkage both achieve loss reductions close to the DIIM benchmark, while backward linkage performs poorly. For the manpower scenario, the gap between cheap methods and DIIM widens significantly, with even the best cheap method (output-weighted linkage) falling substantially short of DIIM's reduction.

This observation motivates the Monte Carlo analysis in Chapter 6: the performance of cheap methods at a single $q_0$ point is insufficient to draw general conclusions. We need to understand how performance varies across the space of possible $q_0$ vectors.

## 5.4 Effect of the Number of Key Sectors

Figure 5.1 shows how the economic loss reduction varies as the number of key sectors $k$ increases, for the COVID-19 scenario. Across all methods, increasing $k$ improves the loss reduction, but the rate of improvement differs. PCA-based selection shows diminishing returns at higher $k$ because PCA's ranking is based on structural importance, which may not align with the sectors most affected by a specific $q_0$.

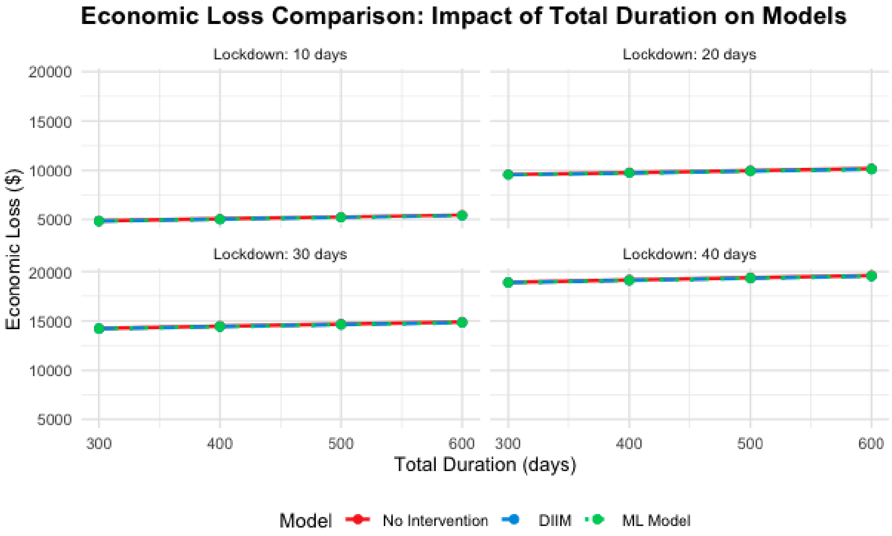


Figure 5.1: Economic loss for different lockdown and total durations (COVID-19).

Figures 5.2 and 5.3 compare the PCA-based and DIIM-based approaches specifically, showing that PCA-based prioritisation can match or exceed DIIM-based prioritisation under the original COVID-19 parameters.

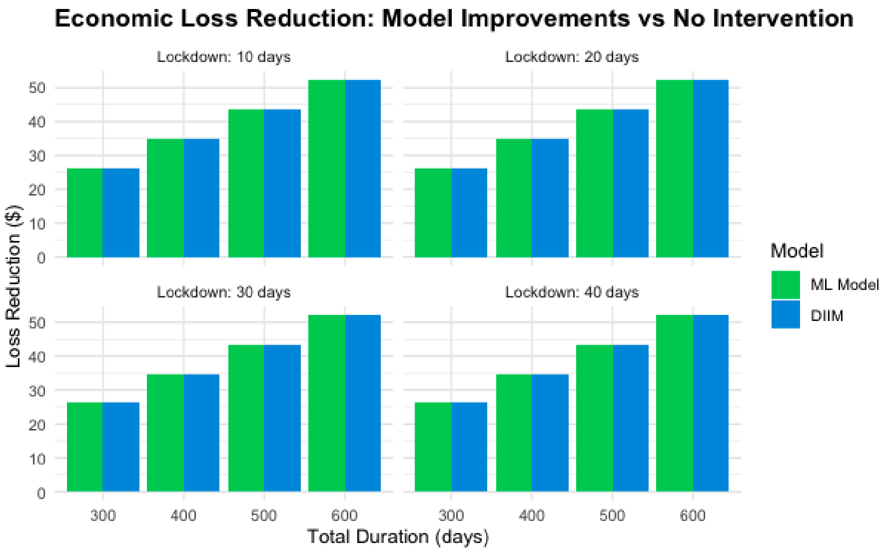


Figure 5.2: Economic loss reduction for PCA vs DIIM (COVID-19).

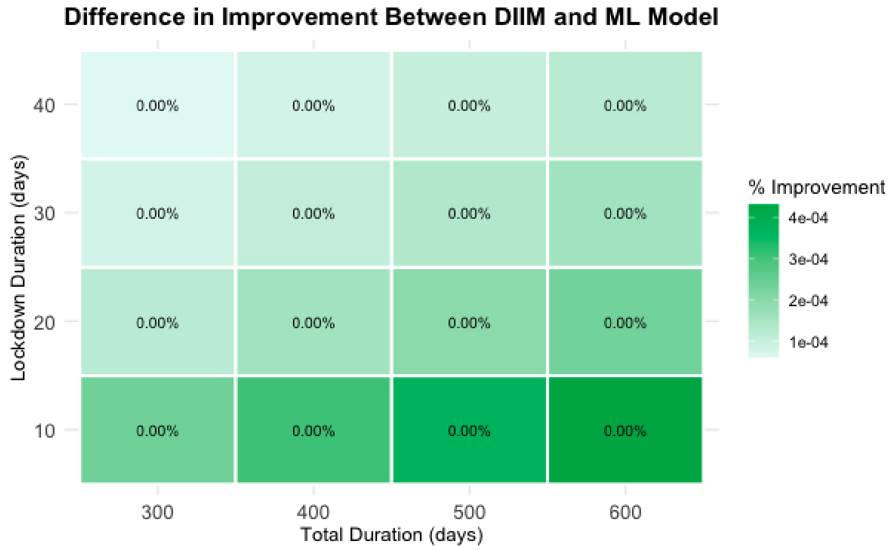


Figure 5.3: Difference in improvement: PCA vs DIIM (COVID-19).

These results demonstrate that PCA can perform well at the original COVID-19 data point, but the question remains: does this hold across a wider range of disruption profiles? This is addressed in the next chapter.

# Chapter 6

# Decision Rules: When Can Cheap Methods Substitute for DIIM?

The previous chapter showed that cheap methods can match DIIM at specific $q_0$ points but not universally. This chapter develops a systematic framework to determine *when* each cheap method can be trusted, using Monte Carlo simulation and logistic regression.

## 6.1 Framework

### 6.1.1 Motivation

All cheap methods produce a *fixed* sector ranking—they depend only on the IO table structure $(A, x)$, not on the disruption profile $(q_0)$. The DIIM, by contrast, adapts its ranking to the specific $q_0$. A cheap method performs well when its fixed ranking happens to align with where $q_0$ concentrates; it fails when the disruption hits sectors that the cheap method did not prioritise.

This insight suggests that the effectiveness of a cheap method is predictable from features of $q_0$. If we can identify these features, we can construct decision rules: "Use cheap method $m$ if [condition on $q_0$]; otherwise, run the full DIIM."

### 6.1.2 Performance Metric

For each cheap method $m$ and a given $q_0$, we compute the performance ratio from Equation (2.24). Method $m$ is considered "close enough" if $R_m \geq 0.95$.

## 6.2 Monte Carlo Simulation

We draw 2 000 random $q_0$ vectors for each scenario (COVID-19, 15 sectors; Manpower, 107 sectors). For each trial:

1. Draw $q_{0,i} \sim \mathrm{Uniform}(10^{-6}, 2\max(q_0^{\text{actual}}))$ independently for each sector $i$.
2. Run the DIIM baseline (no intervention) and compute total economic loss.
3. Run the DIIM with intervention in the DIIM's top-5 sectors (10% $q_0$ reduction) and compute $\Delta EL_{\text{DIIM}}$.
4. For each cheap method $m$, run the DIIM with intervention in method $m$'s top-5 sectors and compute $\Delta EL_m$.
5. Compute $R_m = \Delta EL_m / \Delta EL_{\text{DIIM}}$ and record whether $R_m \geq 0.95$ ("close").

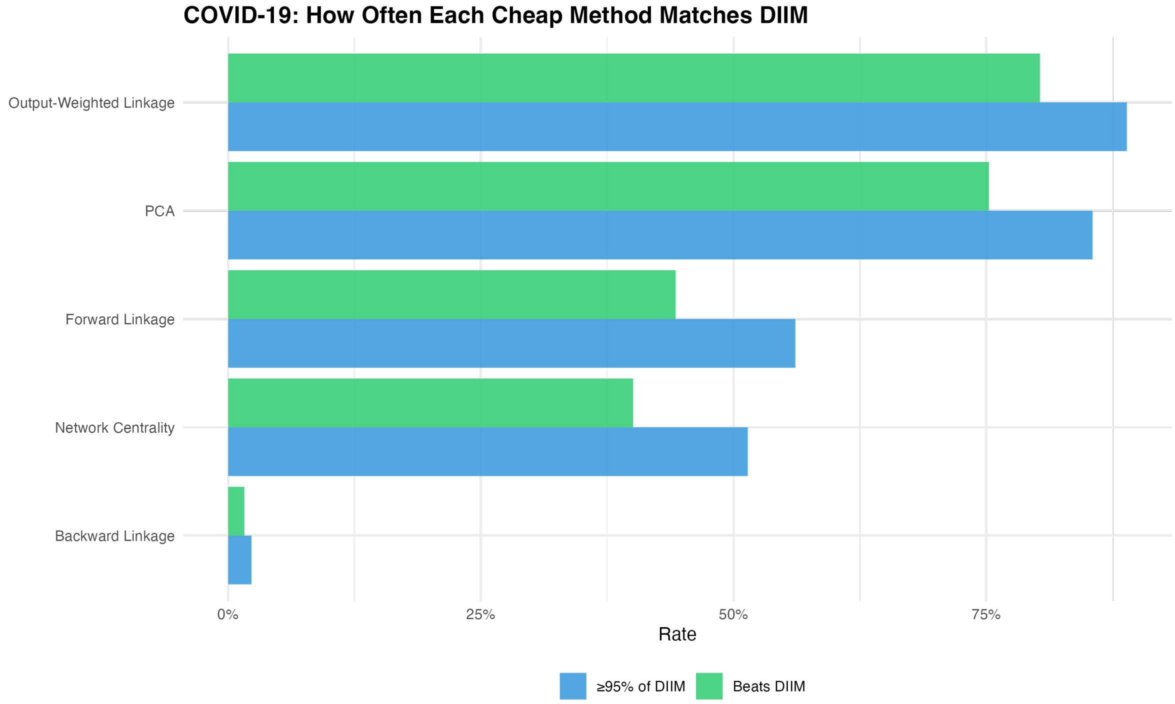


Figure 6.1: Close rates and win rates for each cheap method (COVID-19).

## 6.3 COVID-19 Results

Table 6.1 summarises the Monte Carlo results for the COVID-19 scenario.

| Method | Close Rate (≥95%) | Win Rate | Mean Ratio |
|---|---|---|---|
| Output-Weighted Linkage | 88.9% | 80.3% | 1.156 |
| PCA | 85.5% | 75.2% | 1.095 |
| Forward Linkage | 56.1% | 44.2% | 0.945 |
| Network Centrality | 51.4% | 40.1% | 0.986 |
| Backward Linkage | 2.3% | 1.6% | 0.478 |

Table 6.1: Monte Carlo results for COVID-19 (2 000 trials, $k = 5$).

Output-weighted linkage and PCA both achieve close rates above 85%, with mean performance ratios exceeding 1 (i.e., they *outperform* DIIM on average). This occurs because these methods capture structural importance that sometimes identifies sectors the DIIM's loss-based ranking misses.

Figure 6.2 shows the distribution of performance ratios across the 2 000 trials. Output-weighted linkage and PCA have distributions centred above 1, while backward linkage is centred below 0.5.

## 6.4 Manpower Results

Table 6.2 summarises the manpower scenario results.

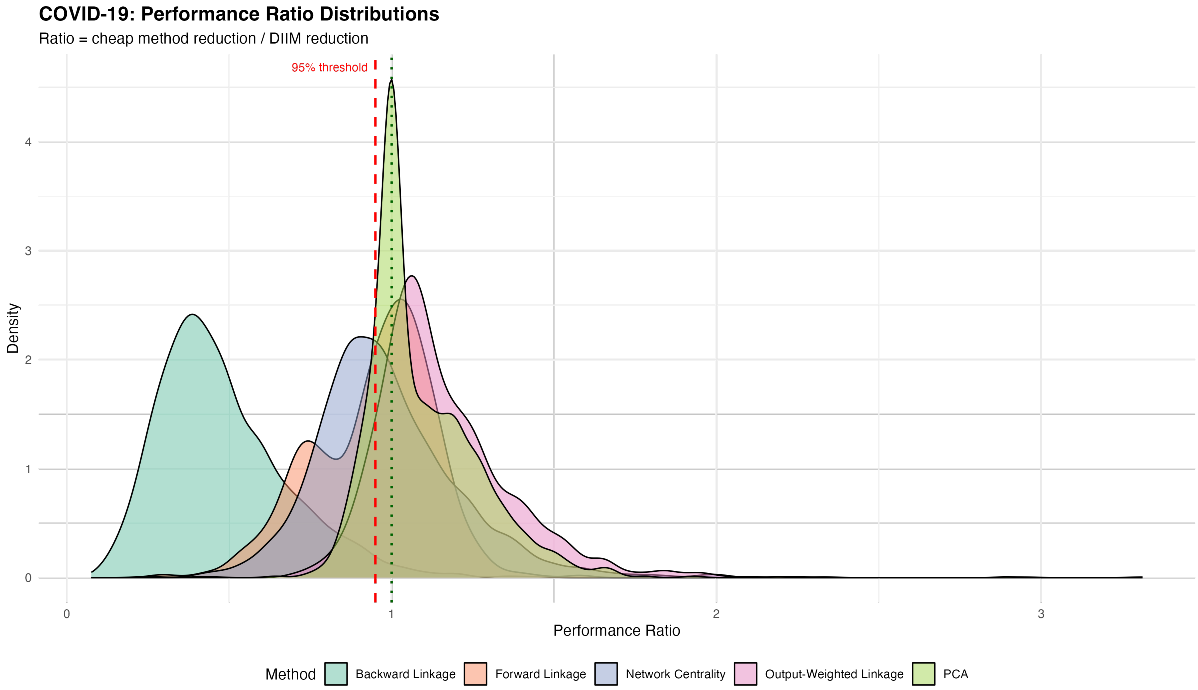


Figure 6.2: Performance ratio distributions (COVID-19).

| **Method** | **Close Rate (≥95%)** | **Win Rate** | **Mean Ratio** |
|---|---|---|---|
| Output-Weighted Linkage | 55.4% | 24.3% | 0.942 |
| Forward Linkage | 8.6% | 0.9% | 0.822 |
| PCA | 5.3% | 0.4% | 0.802 |
| Network Centrality | 1.1% | 0.0% | 0.641 |
| Backward Linkage | 0.0% | 0.0% | 0.175 |

Table 6.2: Monte Carlo results for Manpower (2 000 trials, $k = 5$).

The manpower scenario is much harder for all cheap methods. PCA's close rate drops from 85.5% (COVID-19) to 5.3% (manpower). Even output-weighted linkage, the best performer, only matches DIIM 55% of the time. This is fundamentally driven by the number of sectors: with 107 sectors, the top-5 represent only 4.7% of the economy, and the probability that any fixed ranking captures the five most impactful sectors under a random $q_0$ is much lower.

## 6.5 Decision Rules via Logistic Regression

For each method $m$, we fit a logistic regression model:

$$\log \frac{P(R_m \geq 0.95)}{1 - P(R_m \geq 0.95)} = \beta_0 + \beta_1 f_1 + \beta_2 f_2 + \cdots \tag{6.1}$$

where the features $f_1, f_2, \ldots$ are derived from $q_0$ and the method's sector rankings:

- **Method share**: the fraction of total $q_0$ captured by the method's top-5 sectors.
- **Method average rank**: the mean rank of the method's top-5 sectors in the $q_0$ ranking (normalised to [0,1]).
- **Overlap**: the number of the method's top-5 sectors that also appear in $q_0$'s top-5.

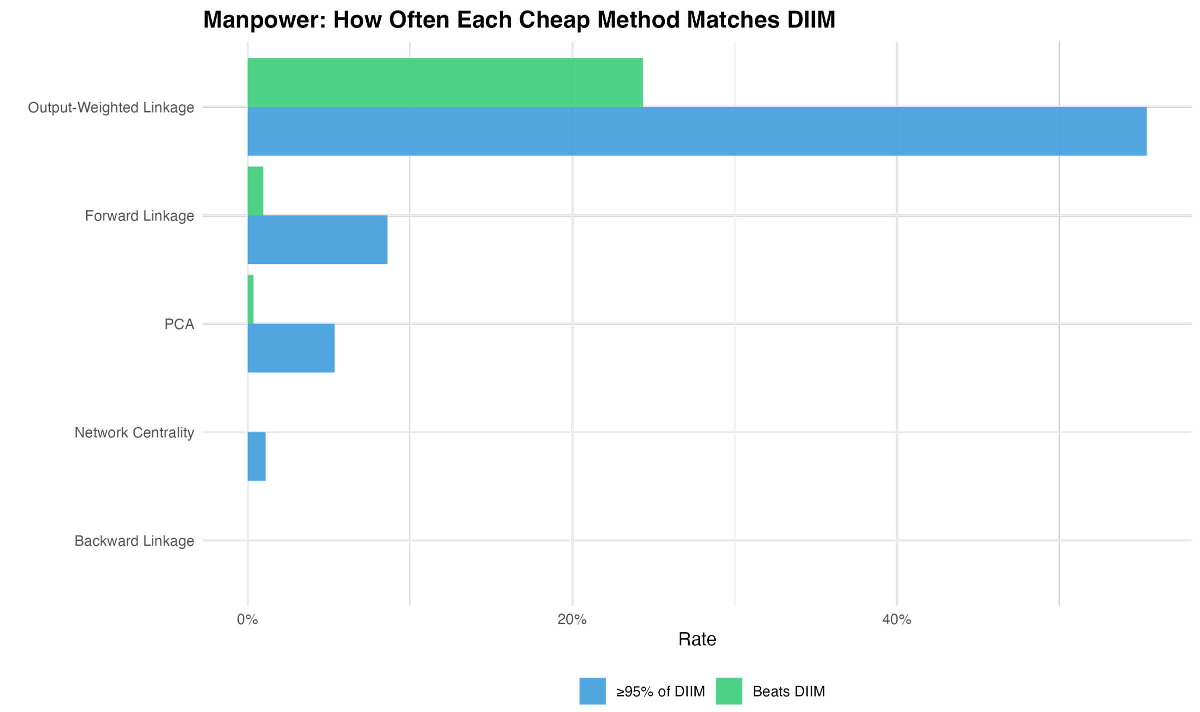


Figure 6.3: Close rates and win rates for each cheap method (Manpower).

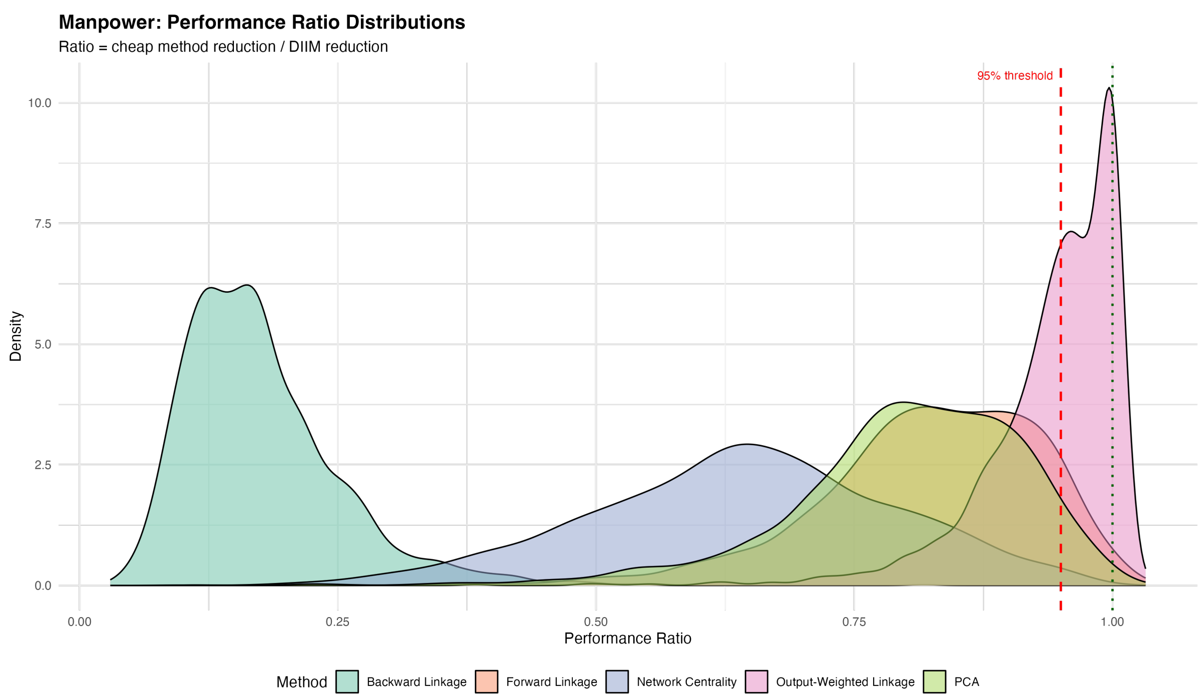


Figure 6.4: Performance ratio distributions (Manpower).

- **General $q_0$ features**: Gini coefficient, coefficient of variation, max-to-mean ratio, and normalised entropy of $q_0$.

For each model, we identify the most significant predictor and compute the Youden's $J$ optimal threshold—the threshold that maximises sensitivity plus specificity minus 1.

Table 6.3 presents the derived decision rules.

| Scenario | Method | Decision Rule | $J$ |
|---|---|---|---|
| COVID-19 | Output-Weighted | OWL_avgrank $< 0.533$ | 0.411 |
| | PCA | PCA_avgrank $< 0.578$ | 0.304 |
| | Network Cent. | NC_overlap $> 0.200$ | 0.197 |
| Manpower | PCA | PCA_share $> 0.057$ | 0.559 |
| | Forward Linkage | FL_avgrank $< 0.456$ | 0.503 |
| | Output-Weighted | OWL_overlap $> 0$ | 0.102 |

Table 6.3: Decision rules with Youden's $J$-optimal thresholds.

The decision rules follow a common pattern: a cheap method works well when the disruption ($q_0$) is concentrated in sectors that the method has already identified as structurally important. The "share" and "average rank" features capture this alignment.

## 6.6 Practical Recommendations

Based on the analysis, we propose the following practical guidelines:

1. **For small economies ($\leq$ 20 sectors)**: Output-weighted linkage or PCA can be used as primary screening tools. With close rates above 85%, the risk of significant underperformance is low.

2. **For large economies ($>$ 50 sectors)**: Output-weighted linkage should be used as a first-pass screen. If the overlap between its top-$k$ sectors and the observed high-$q_0$ sectors is low, the full DIIM should be run.

3. **Pre-event planning**: Since $q_0$ is unknown before a disruption occurs, cheap methods are valuable for *pre-positioning* resources. Output-weighted linkage provides the best structural estimate of which sectors are likely to be critical across a range of disruption profiles.

4. **During a crisis**: Once $q_0$ is observed, the decision rules in Table 6.3 can be evaluated instantly to determine whether the cheap method's recommendation is trustworthy for the specific disruption at hand.

# Chapter 7

# Discussion

## 7.1 Cross-Scenario Comparison

The two case studies reveal a clear pattern: the effectiveness of cheap key sector identification methods depends critically on the number of sectors and the structure of the IO table.

- **COVID-19 (15 sectors)**: Both output-weighted linkage (89%) and PCA (86%) achieve close rates above 85%. With only 15 sectors, the top-5 represent one-third of the economy, and the structural ranking of the IO table is a reasonable approximation of which sectors will be most impacted under a wide range of disruption profiles.
- **Manpower (107 sectors)**: Even the best cheap method (output-weighted linkage, 55%) matches DIIM only about half the time. With 107 sectors, the top-5 represent less than 5% of the economy, and the probability that any fixed structural ranking captures the specific sectors most affected by a given $q_0$ is much lower.

This suggests a fundamental *dimensionality effect*: as the number of sectors grows, the space of possible $q_0$ vectors expands exponentially, making it harder for a fixed ranking to remain robust.

## 7.2 Why Output-Weighted Linkage Outperforms PCA

Output-weighted linkage (OWL) consistently outperforms PCA across both scenarios. This can be understood through two mechanisms:

1. **Economic size matters**: OWL explicitly incorporates sector output ($x_i$), ensuring that structurally important *but economically small* sectors are not over-ranked. PCA, by contrast, operates on the normalised $H$ matrix and can assign high importance to sectors that are structurally central but economically minor.
2. **Dual linkage capture**: OWL combines both backward and forward linkages, capturing both demand-pull and supply-push effects. PCA's eigenvectors blend these effects implicitly but may not weight them optimally for loss reduction.

## 7.3 The Role of $q_0$ Concentration

The logistic regression analysis reveals that the most predictive feature across methods is the *alignment* between the method's fixed ranking and the disruption profile:

- **Methods share** (fraction of $q_0$ in top-$k$ sectors): When the disruption is concentrated in sectors that the cheap method ranks highly, the method trivially works well.

- **Average rank**: When the cheap method's top-$k$ sectors have low average rank in $q_0$ (i.e., they are among the most disrupted), the method performs well.

The practical implication is that the decision rules can be evaluated rapidly: once $q_0$ is observed, computing the share and overlap features requires only a lookup against the pre-computed structural rankings.

## 7.4 National Security Implications

From a national security perspective, the results support a two-stage approach to economic resilience planning:

1. **Peacetime (pre-event)**: Use output-weighted linkage to identify sectors that are structurally critical and economically significant. These sectors should receive priority in resilience investments (e.g., stockpiling, training local replacements, diversifying supply chains) regardless of the specific disruption scenario.
2. **Crisis response**: Once the nature of the disruption is known (i.e., $q_0$ is observed), evaluate the decision rules. If the cheap method's conditions are met, use its recommendations immediately. If not, run the full DIIM for a more accurate assessment. This reduces response time in the critical early hours of a crisis.

For Singapore specifically, the analysis suggests that sectors with high foreign worker concentration *and* strong IO linkages (e.g., construction, certain manufacturing sub-sectors) should be priority targets for workforce resilience measures. Even crude structural analysis using only the IO table can identify these sectors with reasonable accuracy.

## 7.5 Limitations

Several limitations should be noted:

1. **Uniform intervention**: All methods are compared using a standardised 10% reduction in $q_0$ for top-$k$ sectors. In practice, the feasible intervention magnitude may vary across sectors.
2. **Fixed $k$**: The analysis primarily uses $k = 5$. Different values of $k$ may alter the relative performance of methods.
3. **IO table vintage**: The COVID-19 scenario uses the 2019 IO table and the manpower scenario uses the 2022 IO table. Structural changes between these years are not controlled for.
4. **Recovery dynamics**: The DIIM assumes exponential recovery with fixed resilience coefficients. In practice, recovery may be non-exponential, sector-specific, and dependent on policy interventions.
5. **$q_0$ distribution**: The Monte Carlo analysis uses uniform random $q_0$ vectors. Real disruptions may have structured $q_0$ vectors (e.g., concentrated in specific industry groups).

## 7.6 Future Work

Future extensions could include:

- Incorporating structured $q_0$ distributions (e.g., sector-correlated disruptions) in the Monte Carlo analysis.

- Testing whether ensemble methods (combining multiple cheap method rankings) improve close rates.
- Extending the framework to multi-period disruptions where $q_0$ evolves over time.
- Validating the decision rules on actual disruption data from other economies.

# Chapter 8

# Conclusion

This project developed and applied a quantitative framework for assessing economic resilience under disruption, with direct relevance to Singapore's national security planning.

Using the Dynamic Inoperability Input-Output Model (DIIM), two disruption scenarios were studied. The COVID-19 pandemic scenario (15 sectors, 2019 IO table) demonstrated how lockdown-induced workforce unavailability cascaded through input-output linkages to produce sector-level inoperability paths and cumulative economic losses. The manpower disruption scenario (107 sectors, 2022 IO table), motivated by the risk of grey zone conflicts triggering foreign worker departures, revealed stronger cascading effects in a denser production network under purely structural disruption ($c^* = 0$).

A central contribution of this study is the systematic comparison of five cheap structural methods for identifying key sectors against the DIIM benchmark. Output-weighted linkage—which combines the Leontief inverse's linkage measures with sector output—emerged as the best cheap substitute, achieving close-to-DIIM performance in 89% of randomised disruptions for the 15-sector scenario and 55% for the 107-sector scenario. PCA performed well for the smaller economy (86%) but dropped to 5% for the larger one, revealing a dimensionality effect: as the number of sectors grows, fixed structural rankings become less reliable substitutes for simulation-based identification.

Decision rules were derived using logistic regression on $q_0$-derived features, providing policymakers with a practical tool: given observable characteristics of the disruption, determine instantly whether a cheap method's recommendation is trustworthy or whether the full DIIM should be run. For national security planning, this enables a two-stage approach—using structural analysis for peacetime resilience investments, and the decision rules for rapid crisis-time assessment.

The framework is generalisable beyond the two scenarios studied here. Any economy with an available IO table can compute the cheap structural rankings in peacetime and apply the decision rules when a disruption occurs. Future work could extend the approach to correlated disruptions, multi-period dynamics, and ensemble methods that combine multiple cheap rankings for improved robustness.

# Bibliography


[1] Joost R. Santos and Yacov Y. Haimes. Modeling the demand reduction input-output (i-o) inoperability due to terrorism of interconnected infrastructures. *Risk Analysis*, 24(6):1437–1451, 2004.

[2] Jian Jin and Haoran Zhou. A demand-side inoperability input–output model for strategic risk management: Insight from the COVID-19 outbreak in shanghai, china. *Sustainability*, 15(5):4003, 2023.

[3] Ministry of Manpower, Singapore. Foreign workforce numbers. https://www.mom.gov.sg/documents-and-publications/foreign-workforce-numbers, 2023. Accessed 2026-02-17.

[4] Ministry of Health, Singapore. End of circuit breaker, phased approach to resuming activities safely. https://www.moh.gov.sg/newsroom/end-of-circuit-breaker-phased-approach-to-resuming-activities-safely/, May 2020. Newsroom release dated 19 May 2020. Accessed 2026-02-17.

[5] Ministry of Health, Singapore. Post circuit breaker measures. https://www.moh.gov.sg/newsroom/post-circuit-breaker-measures/, 2020. Newsroom / Parliamentary reply page referencing circuit breaker dates. Accessed 2026-02-17.

[6] Ministry of Defence, Singapore. Factsheet: Singapore's total defence. https://www.mindef.gov.sg/web/portal/mindef/defence-matters/defence-topic/defence-topic-detail/total-defence, 2020. Total Defence overview including economic, digital, and military defence pillars. Accessed 2026-02-17.

[7] SINGSTAT (Singapore Department of Statistics). Industry by industry input-output table (supply, use and input-output tables 2019). https://data.gov.sg/datasets/d_959da3e78690cb3136c529fbc448d178/view. data.gov.sg dataset. Accessed 2026-02-17.

[8] Yacov Y. Haimes. The surrogate worth trade-off method. *Developments in Water Science*, 3:34–57, 1975.

# Appendix A: COVID-19 Scenario Data

| Sector ID | PC1 | PC2 |
|---|---|---|
| 3 | 0.772976374 | -0.158540904 |
| 2 | 0.488575487 | 0.547564001 |
| 5 | 0.230631604 | 0.602425551 |
| 8 | 0.173952844 | 0.31984955 |
| 4 | 0.16376151 | 0.197548491 |
| 10 | 0.141148665 | 0.185477914 |
| 7 | 0.107051197 | 0.232037887 |
| 11 | 0.100445788 | 0.154054165 |
| 1 | 0.082357584 | 0.203204452 |
| 9 | 0.065932369 | 0.120308858 |
| 12 | 0.02097817 | 0.033819003 |
| 6 | 0.01904942 | 0.04009044 |
| 15 | 0.010160651 | 0.015616709 |
| 14 | 0.004471868 | 0.006256627 |
| 13 | 0.002201633 | 0.00402146 |

Table 8.1: Sector PCA loadings (COVID-19, 15 sectors)

| | Agriculture, Fishing, Quarrying, Utilities and Sewerage & Waste Management | Manufacturing | Construction |
|---|---|---|---|
| Agriculture, Fishing, Quarrying, Utilities and Sewerage & Waste Management | 4,308.828700 | 2,985.482100 | 198.954100 |
| Manufacturing | 498.915600 | 59,777.284000 | 4,939.792300 |
| Construction | 166.973900 | 498.152500 | 23,583.027800 |

Table 8.2: Cross-section of technical coefficient matrix (COVID-19)

| Sector ID | Sector | Initial inoperability |
|---|---|---|
| 1 | Agriculture, Fishing, Quarrying, Utilities and Sewerage & Waste Management | 0.002563 |
| 2 | Manufacturing | 0.000752 |
| 3 | Construction | 0.006890 |
| 4 | Wholesale & Retail Trade | 0.001639 |
| 5 | Transportation & Storage | 0.001107 |
| 6 | Accommodation & Food Services | 0.008462 |
| 7 | Information & Communications | 0.001936 |
| 8 | Financial & Insurance Services | 0.001091 |
| 9 | Real Estate Services | 0.000765 |
| 10 | Professional Services | 0.003087 |
| 11 | Administrative & Support Services | 0.005325 |
| 12 | Public Administration & Education | 0.002954 |
| 13 | Health & Social Services | 0.003429 |
| 14 | Arts, Entertainment & Recreation | 0.004552 |
| 15 | Other Community, Social & Personal Services | 0.015819 |

Table 8.3: Sector Initial Inoperability (COVID-19)

# Appendix B: Manpower Scenario Data

The manpower disruption scenario uses the 2022 Singapore IO table with 107 sectors. Due to the large number of sectors, only summary statistics are presented here.

| **Parameter** | **COVID-19** | **Manpower** |
|---|---|---|
| Number of sectors ($n$) | 15 | 107 |
| IO table year | 2019 | 2022 |
| Mean initial inoperability | 0.00398 | varies |
| Max initial inoperability | 0.01582 | varies |
| Demand shock ($c^*$) | $> 0$ | $= 0$ |
| Lockdown duration | 55 days | 55 days |
| Total horizon | 751 days | 751 days |
| PCA top-5 sectors | 3, 2, 5, 8, 4 | 17, 57, 69, 54, 62 |
| DIIM top-5 sectors | by simulation | by simulation |

Table 8.4: Summary of scenario parameters

# Appendix C: Code

The R code for all simulations and analyses is available in the project repository. Key scripts include:

- `functions.R`: Core DIIM function, data loading, simulation comparison
- `pca.R`: PCA analysis on the integrated IO matrix
- `simulations/decision_rules.R`: Monte Carlo framework, logistic regression, decision rules
- `simulations/enhanced_comparison.R`: Multi-PC PCA and variable top-$k$ sweep
- `simulations/alternative_methods.R`: Network centrality, sensitivity analysis, hybrid methods
- `manpower-disruption/manpower-disruption.R`: Manpower scenario DIIM simulation